Temperature-Dependent Properties of Telechelic Hydrophobically Modified Poly(*N*-isopropylacrylamides) in Water: Evidence from Light Scattering and Fluorescence Spectroscopy for the Formation of Stable Mesoglobules at Elevated Temperatures

Piotr Kujawa,[†] Fumihiko Tanaka,[‡] and Françoise M. Winnik*,[†]

Department of Chemistry and Faculty of Pharmacy, University of Montreal, CP 6128 Succursale Centre Ville, Montreal, Quebec, Canada H3C 3J7, and Department of Polymer Chemistry, Kyoto University, Katsura, Nishikyo-ku, Kyoto 615-8510, Japan

Received January 4, 2006; Revised Manuscript Received February 13, 2006

ABSTRACT: The self-assembling properties of hydrophobically modified (HM) telechelic poly(*N*-isopropylacrylamides) (PNIPAM) were studied in aqueous solutions of concentration ranging from 0.1 to 11 g L^{-1} by fluorescence spectroscopy, using *N*-phenyl-1-naphthylamine as a probe, and by static (SLS) and dynamic (DLS) light scattering over a temperature domain encompassing their cloud point (T_{cp}) and coil-to-globule transition temperature (T_M). The telechelic HM−PNIPAM samples bear *n*-octadecyl termini, and their molar mass (M_n) ranges from 12 000 to 49 000 g mol^{-1} with a polydispersity index lower than 1.20. In cold aqueous solution, the HM−PNIPAM samples associate in the form of flower micelles ($10.8 < R_H < 17.5$ nm, $R_G/R_H \cong 1.3-1.5$) consisting of ≅16−27 polymer chains, depending on their molecular weight. In solutions heated under equilibrium conditions above T_M, individual flower micelles with collapsed loops associate to form stable mesoglobules ($R_G/R_H \sim 0.80$) comprising a few hundreds chains with a more rigid and more polar interior than the hydrophobic core of hydrated flower micelles. The size of the mesoglobules increases with increasing polymer concentration ($19 < R_H < 115$ nm), but in all cases the mesoglobule size distributions are narrower than those of the corresponding polymer micelles in cold solutions.

Introduction

The assembly of associative polymers in water has attracted widespread attention over the past decades, as it is at the root of many practical applications of waterborne fluids, such as paints, coating formulations, cosmetics, and foodstuffs.[1−3] This group of polymers includes thickeners, such as polyacrylates, cellulose derivatives, and hydrophobic ethylene oxide−urethane copolymers (HEUR), which consist of a hydrophilic ethylene oxide chain carrying hydrophobic termini.[4] A characteristic feature of HEUR copolymers in water is their ability to form flower micelles via attraction of their hydrophobic end groups.[5,6] When the polymer concentration exceeds the critical overlap concentration of flowers, connectivity through bridging EO chains takes place progressively, resulting, on the macroscopic scale, in an abrupt rise in solution viscosity.[7,8] The conformation and association of HEUR copolymers in a solvent selective for the backbone have been subjected to various theoretical investigations and experimental studies.[9−11] Most studies aim to determine, or predict, parameters such as the critical concentration of the onset of micellization (c_{mic}), the micelle aggregation number (N_{agg}), or number of chains forming individual flowers in solutions of low concentration, and the critical overlap concentration for which micelle connectivity is initiated.[12,13] Effects of temperature and ionic strength on micellization have been assessed, together with the influence of structural parameters of the polymers themselves, such as chain length, end-group length, and chemical composition.[14−18]

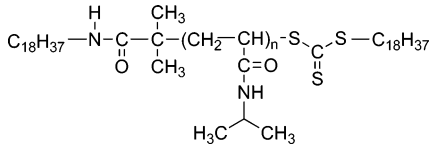

Figure 1. Chemical structure of the polymers investigated.

We reported recently the preparation of an associative polymer consisting of an *N*-isopropylacrylamide (NIPAM) chain of $M_n \cong 35\,000$ g mol^{-1} carrying an *n*-octadecyl group at each chain end (C_{18}-PNIPAM-C_{18}, Figure 1).[19] On the basis of data from light scattering and fluorescence spectroscopy measurements coupled with dynamic oscillatory tests carried out with aqueous solutions of this telechelic hydrophobically modified HM−PNIPAM, we concluded that the association of C_{18}-PNIPAM-C_{18} in water exhibits patterns typical of HEUR copolymers: formation of flower micelles in solutions of low concentration and, above a critical concentration, intermicellar bridging leading to clusters of micelles and, eventually, to a cross-linked micellar network.[19]

Subsequently, we prepared a set of telechelic HM-PNIPAM ranging in size from $M_n \cong 12\,000$ to ≅ 50 000 g mol^{-1}, and examined via microcalorimetry and turbidimetry the effect of temperature on solutions of these polymers.[20] It is useful to remember that the homopolymer, PNIPAM, is soluble in cold water at all concentrations, but its aqueous solutions phase-separate once they are heated above ≅32 °C.[21] The macroscopic phase separation of aqueous PNIPAM reflects the release of water molecules from the polymer hydration layer into bulk water, the collapse of denuded polymer chains into globules, and the aggregation of individual globules into larger objects.[22] Attaching hydrophobic end groups to a PNIPAM chain has several consequences. The miscibilityof telechelic HM−

[†] University of Montreal.
[‡] Kyoto University.
* Corresponding author: Ph (514) 340 5179; Fax (514) 340 3245; e-mail francoise.winnik@umontreal.ca.

10.1021/ma0600254 CCC: $33.50
Published on Web 03/23/2006

Table 1. Physical Properties of the Polymers Investigated[a]

polymer	M_n[b]	M_w/M_n[b]	n	T_M[c]/°C
C_{18}-PNIPAM-C_{18}-49K	49 000	1.20	428	33.2
C_{18}-PNIPAM-C_{18}-22K	22 200	1.16	191	32.2
C_{18}-PNIPAM-C_{18}-12K	12 400	1.11	104	31.1

[a] M_n and M_w: number- and weight-average molecular weight, respectively; n: polymerization degree; T_M: phase transition temperature. [b] From GPC analysis (see ref 20). [c] From microcalorimetry (polymer concentration: 0.3 g L^{-1}, see ref 20).

PNIPAMs with water is poorer than that of PNIPAM, as a result of direct interactions between water molecules and the alkyl chains. The mixing entropy of the polymer chains is reduced as well due to the increase of their apparent molecular weight via micelle formation. Both factors favor phase separation, so that the lower critical solution temperature or solution cloud point (T_{cp}) tends to shift to temperatures lower than the T_{cp} of PNIPAM. The hydration of the main chain is not affected as much by the association of the termini, since the polymer chains remain exposed to water even when association takes place, except for segments near the micellar core. Thus, as is the case for PNIPAM, an increase in temperature triggers the coil-to-globule collapse of the micelle loops, a phenomenon which occurs at a temperature T_M which is close to the value recorded for PNIPAM itself and is only slightly dependent on molecular weight.[20]

We present here a light scattering and fluorescence spectroscopy study of aqueous solutions of the same set of telechelic HM−PNIPAMs (Table 1) heated through their cloud point and through the temperature of the coil-to-globule collapse of PNIPAM chains. Theoretical[23] and computational[24,25] studies of chain collapse followed by intermicellar association have been reported by Timoshenko et al., who focused on the formation of stable mesoglobules defined as multichain globules which possess a well-characterized size distribution, but not necessarily a well-defined conformational structure. These studies by Gaussian variational theory and by lattice Monte Carlo simulation demonstrate that, within a limited concentration range, mesoglobules of equal size or of narrow size distribution are a thermodynamically stable state of lowest free energy. We employ dynamic and static laser light scattering to gain information on the size and aggregation number of the polymeric micelles formed in cold aqueous solutions and monitor their fate as a function of increasing temperature. Static fluorescence measurements were carried out with telechelic HM−PNIPAMs aqueous solutions containing small amounts of *N*-phenyl-1-naphthylamine (PNA) to determine the onset of micellization. Fluorescence depolarization studies were conducted as well to assess the microviscosity of the hydrophobic core of hydrated micelles and of collapsed globules formed at elevated temperatures. The results are discussed in the context of the current understanding of the association of telechelic amphiphilic copolymers and the stability of mesoglobules of thermoresponsive polymers in dilute aqueous solutions above their cloud point.

Experimental Section

Materials. Water was deionized with a Millipore Milli-Q system. All other solvents were reagent grade and used as received. The nonionic surfactants Brij 76, 78, and 700 ($C_{18}H_{37}(OCH_2CH_2)_nOH$ where $n \cong 10$, 20, and 100, respectively), *N*-phenyl-1-naphthylamine (PNA), and *n*-octadecanol were purchased from Aldrich Chemicals and used without further purification. The telechelic HM−PNIPAM samples were prepared and characterized as described previously.[20] Their molecular characteristics are listed in Table 1. The sample of unmodified PNIPAM used in control experiments PNIPAM-31K (M_n = 31 000 g mol^{-1}, PDI = 1.78) was obtained by standard free radical polymerization in dioxane.[20]

Fluorescence Measurements. Steady-state fluorescence spectra were recorded either on a SPEX Industries Fluorolog 212 spectrometer equipped with a GRAMS/32 data analysis system for measurements carried out at 20 °C (slit settings: excitation 1.0 mm and emission 0.5 mm) or on a Varian Cary Eclipse spectrometer for temperature-dependent measurements, using a water-jacketed cell holder connected to a Cary circulating water bath. The temperature of the sample fluid was measured with a thermocouple immersed in a water-filled cell placed in one of the four cell holders in the sample compartment. The slit settings were 10 and 2.5 nm for excitation and emission, respectively. Emission spectra were recorded with an excitation wavelength of 340 nm. They were not corrected. In the case of temperature-dependent experiments, the temperature of the sample kept in the insulated instrument cell compartment was changed stepwise as follows: at the end of scans performed at a given temperature setting, the solution was heated to the temperature of the next measurement at a constant heating rate (ca. 1 °C/min). It was then kept at this temperature for 60 min prior to measurement.

Fluorescence anisotropy values (r) were determined with a Varian Cary spectrometer Eclipse fitted with two Glan-Thompson polarizers in the L-format configuration. The slits were set at 10 and 2.5 nm for excitation and emission, respectively. The excitation wavelength was 340 nm. The fluorescence anisotropy was calculated from the relationship

$$r = \frac{I_{VV} - GI_{VH}}{I_{VV} + 2GI_{VH}} \quad (1)$$

where $G = I_{VH}/I_{HH}$ is an instrumental correction factor and I_{VV}, I_{VH}, and I_{HH} refer to the resultant emission intensities at 410 nm polarized in the vertical or horizontal planes (second subindex) upon excitation with either vertically or horizontally polarized light (first subindex). The anisotropy is a measure of the effective viscosity of the probe environment (microviscosity).[26]

Solutions for fluorescence analysis were prepared from aqueous polymer stock solutions (11.0 g L^{-1}). The concentration of the fluorescent probe, PNA, in the samples was fixed at 5 μM. Solutions were not degassed prior to measurements.

Light Scattering (LS) Experiments. Static (SLS) and dynamic (DLS) light scattering experiments were performed on a CGS-3 goniometer (ALV GmbH) equipped with a ALV/LSE-5003 multiple-τ digital correlator (ALV GmbH), a He−Ne laser (λ = 632 nm), and a C25P circulating water bath (Thermo Haake). The temperature was set at 20 °C, unless otherwise stated. Solutions for analysis were prepared by dilution of aqueous polymer stock solutions (11.0 g L^{-1}) allowed to equilibrate under gentle stirring for at least 12 h. The diluted solutions (0.1−5 g L^{-1}) were kept at room temperature for at least 12 h after preparation. Prior to the measurements, the solutions were filtered directly into the light scattering cells through 0.45 and 0.22 μm Millex Millipore PVDF membranes. Temperature-dependent measurements were carried our following the same heating protocole as in the case of fluorescence experiments (see above).

SLS experiments yield the weight-average molar mass (M_w) and the *z*-average root-mean-square radius of gyration (R_G) of scattering objects in dilute solution, based on the angular dependence of the excess absolute scattering intensity, known as the excess Rayleigh ratio $R(q,c)$ given by eq 2:

$$\frac{K(c - c_{mic})}{R(q,c)} \cong \frac{1}{M_w P(\Theta)} + 2A_2(c - c_{mic}) \quad (2)$$

where c is the polymer concentration, c_{mic} is the concentration of micellization onset, q is the scattering vector ($q = (4\pi n/\lambda) \sin(\Theta/2)$), A_2 is the second virial coefficient, n is the refractive index of the solvent, λ is the wavelength of the light in vacuum, and Θ is the scattering angle (30°−150°). The scattering constant is K =

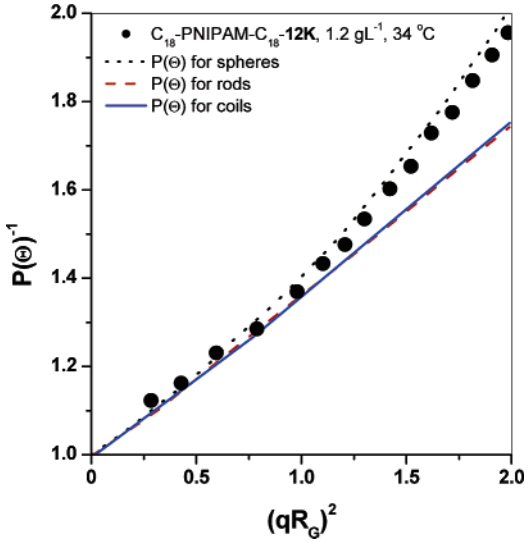

Figure 2. Reciprocal of the theoretical scattering functions for particles of basic shapes as a function of $(qR_G)^2$. The full circles are the values obtained by an analysis assuming a spherical shape of experimental R_G values from a Guinier analysis of measurements carried out in aqueous solutions of C_{18}-PNIPAM-C_{18}-12K, 1.2 g L^{-1}, 34 °C.

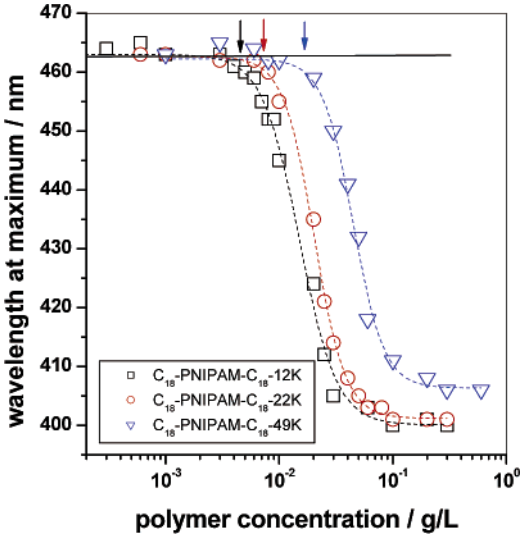

Figure 3. Changes in the wavelength of maximum emission of *N*-phenyl-1-naphthylamine (PNA) in aqueous solutions of three telechelic HM-PNIPAM samples as a function of polymer concentration (temperature: 20 °C, [PNA] = 5 μM). The arrows indicate the concentration corresponding to the onset of micellization (c_{mic}).

$4\pi^2n^2(dn/dc)^2/N_A\lambda^4$, where dn/dc is the refractive index increment and N_A is Avogadro's number. The dn/dc of telechelic HM−PNIPAMs in water was assumed to be independent of temperature and equal to 0.167 mL/g, the value determined for PNIPAM in water. [27] In eq 2, it is assumed that the contribution of a single polymer chain to the scattering intensity is negligible, compared to that of the micelles.

Data recorded from solutions below their phase transition temperature were analyzed according to the Zimm method, assuming that the macromolecules are in a swollen conformation. In this case, the particle scattering function is $P(\Theta) = 1 - (q^2R_G^2)/3$, where R_G is the radius of gyration. Since $(q^2R_G^2)/3 \ll 1$, it may be assumed that $1/[1 - (q^2R_G^2)/3] \cong 1 + (q^2R_G^2)/3$. Thus, eq 2 becomes

$$\frac{K(c - c_{mic})}{R(q,c)} \cong \frac{1}{M_w}\left(1 + \frac{R_G^2}{3}q^2\right) + 2A_2(c - c_{mic}) \qquad (3)$$

The apparent mass of a polymer ($M_{w,app}$) in a solution of concentration c was obtained by extrapolation of the scattered intensity $R(q,c)/(c - c_{mic})$ to $q = 0$. The apparent radius of gyration was obtained by a mean-square linear fit of the inverse of the scattered intensity vs q^2 (see eq 3).

Data recorded for solutions heated above their cloud point were analyzed assuming a hard-sphere conformation of the aggregates. According to Guinier, when $q^2R_G^2 \cong 1$, the radius of gyration of large hard spheres can be approximated from the particle scattering function $P(\Theta) = \exp[-(q^2R_G^2)/3]$. Thus, M_w and R_G can be calculated from eq 4:

$$\frac{K(c - c_{mic})}{R(q,c)} \cong \frac{1}{M_w \exp\left(-\frac{R_G^2q^2}{3}\right)} + 2A_2(c - c_{mic}) \qquad (4)$$

The experimental curve of $P(\Theta)^{-1}$ vs $q^2R_G^2$ recorded for $T > T_M$ are in good agreement with the theoretical curve corresponding to a hard sphere (Figure 2).

In DLS experiments, one measures the normalized time autocorrelation function of the scattered intensity, which can be expressed in terms of the autocorrelation function of the concentration fluctuations. In our experiments, the relaxations had always a diffusive character with a characteristic time (τ) inversely proportional to q^2. A cumulant analysis was applied to obtain the diffusion coefficient (D) of the scattering objects in solution. Extrapolation of the first reduced cumulant $(\tau q^2)^{-1}$ to $q = 0$ yields the value of D, which is related to the average hydrodynamic radius R_H of the scattering objects by eq 6:

$$D = \frac{k_BT}{6\pi\eta_sR_H} \qquad (5)$$

where η_s is the viscosity of the solvent, k_B is the Boltzmann constant, and T is the absolute temperature.

In some cases, the average relaxation time was determined by the CONTIN analysis based on the inverse Laplace transform of the normalized dynamical correlation function of the polymer concentration fluctuations. This method is more appropriate for solutions characterized by several relaxation mechanisms. It was found that the relaxation times obtained using this method coincide, within experimental uncertainties, with those calculated by the cumulant analysis.

Results and Discussion

Aqueous Solutions of Telechelic PNIPAMs below the Phase Transition Temperature. Fluorescence Probe Studies. Fluorescence probes, such as 8-anilino-1-naphthalenesulfonic acid (ANS), *N*-phenyl-1-naphthylamine (PNA), and pyrene, detect the formation of hydrophobic nanodomains in aqueous solutions of surfactants and amphiphilic copolymers.[28−30] It turns out that the trithiocarbonate group is an efficient quencher of the emission of pyrene, the standard probe of micellization. This photophysical property complicates the analysis of fluorescence data recorded for pyrene in aqueous solutions of the telechelic HM−PNIPAMs under scrutiny here. The trithiocarbonate group also quenches the emission of ANS and PNA, but with a lower efficiency.[31] We chose to use PNA, since its solubility in water is much lower than that of ANS. The probe PNA was used successfully to monitor the micellization of surfactants[32,33] and various polymers obtained by RAFT polymerization with trithiocarbonates as chain transfer agents[34] and to determine the solvation properties of PNIPAM.[35]

Emission spectra of PNA in cold aqueous C_{18}-PNIPAM-C_{18} solutions were determined for all samples as a function of polymer concentration. A blue shift of the wavelength of maximum emission, from ≅464 nm in water to ≅405 nm, took place as the polymer concentration exceeded a value of 6−24

Table 2. Characteristics of the Micelles of Various Telechelic HM−PNIPAM Samples in Dilute Aqueous Solutions below Their Cloud Point (20 °C)[a]

		N_{agg}[c]		R_H[d]/nm		R_G[c]/nm	
polymer	c_{mic}[b]/g L^{-1}	1 g L^{-1}	10 g L^{-1}	1 g L^{-1}	10 g L^{-1}	1 g L^{-1}	10 g L^{-1}
C_{18}-PNIPAM-C_{18}-49K	0.024	16 ± 2	22 ± 1	17.5 ± 0.5	26.1 ± 0.8	22.5 ± 0.9	31.6 ± 0.9
C_{18}-PNIPAM-C_{18}-22K	0.010	24 ± 1	32 ± 2	12.9 ± 0.3	22.2 ± 0.5	19.8 ± 0.4	34.9 ± 0.7
C_{18}-PNIPAM-C_{18}-12K	0.006	27 ± 1	39 ± 2	10.8 ± 0.5	17.0 ± 0.8	15.6 ± 0.6	25.5 ± 1.2

[a] c_{mic}: concentration of the onset of micellization; N_{agg}: aggregation number; R_G: radius of gyration; R_H: hydrodynamic radius. [b] From fluorescence probe measurements. [c] From static light scattering measurements. [d] From dynamic light scattering experiments.

Table 3. Wavelength of Maximum Emission (λ_{max}) and Fluorescence Anisotropy (r) of PNA in Aqueous Solutions of Telechelic HM−PNIPAM Micelles (≅0.06 g L^{-1}), PNIPAM (0.06 g L^{-1}), and Model Compounds (1 g L^{-1})

	λ_{max} (nm)		r	
sample	T = 18 °C	T = 35 °C	T = 18 °C	T = 35 °C
C_{18}-PNIPAM-C_{18}-49K	410	416	0.20	0.29
C_{18}-PNIPAM-C_{18}-22K	404	417	0.21	0.31
C_{18}-PNIPAM-C_{18}-12K	403	415	0.23	0.29
PNIPAM-31K	466	416	0.01	0.22
Brij 76, $C_{18}H_{37}(OCH_2CH_2)_{10}OH$	420	420	0.08	0.03
Brij 78, $C_{18}H_{37}(OCH_2CH_2)_{20}OH$	419	419	0.07	0.03
Brij 700, $C_{18}H_{37}(OCH_2CH_2)_{100}OH$	420	420	0.05	0.03

ppm depending on the molecular weight of the polymers, indicating the formation of hydrophobic nanodomains. The shift of λ_{max} occurred over a broad polymer concentration range. The polymer concentration corresponding to the onset of the decrease in λ_{max}, indicated by an arrow in Figure 3, was taken as the polymer concentration for which micellization is initiated (c_{mic}, Table 2). The c_{mic} values, expressed in terms of *n*-octadecyl concentration, are the same for all polymers, ≅(0.90 ± 0.02) μmol L^{-1} $C_{18}H_{37}$. This concentration is approximately the same as that of the fluorescent probe (5 μM). Under these circumstances, one cannot ignore the fact that, as in all methods that use an extrinsic probe, the reporter molecule may influence the event. When PNA is used to detect surfactant micellization, the probe influence on the cmc value can sometimes be detected, leading to an overestimation of the c_{mic}.[32]

The λ_{max} plateau value recorded for polymer solutions of concentration beyond c_{mic}, which reflects the micropolarity sensed by the probe within the hydrophobic core of the micelles, varies slightly as a function of the polymer length (Table 3). It is lower for solutions of C_{18}-PNIPAM-C_{18}-12K and C_{18}-PNIPAM-C_{18}-22K compared to the polymer of highest mass, implying a slight enhancement in the hydrophobicity of the probe environment in micelles formed by the shorter polymer chains. The values are similar to the wavelength of maximum emission of PNA in liquid *n*-octadecanol (λ_{max} = 405 nm, 70 °C). We measured the spectra of PNA in micellar solutions of various neutral surfactants composed of *n*-octadecyl chains and hydrophilic chains consisting of ∼10, 20, or 100 ethylene oxide units (Brij surfactants). The bathochromic shift that accompanies the transfer of PNA from water to their micellar core turned out to be smaller compared to the situation in C_{18}-PNIPAM-C_{18} solutions (λ_{max} ≅ 420 nm, Table 3). Thus, the micellar core of telechelic HM−PNIPAMs is less polar than that of low-molecular-weight surfactants, an indication of a more restricted penetration of water molecules.

The probe entrapped within the flower micelles exhibited relatively high anisotropy values, determined by fluorescence depolarization measurements carried out with polymer solutions above their c_{mic} (Table 3). The anisotropy values do not depend on the length of the polymer chains. They are markedly higher than the values recorded for the same probe in micellar solutions of Brij surfactants bearing *n*-octadecyl chains (Table 3), an indication that the core of the polymeric micelles is less fluid than that of surfactant micelles, as reported previously for other HM polymers.[36,37]

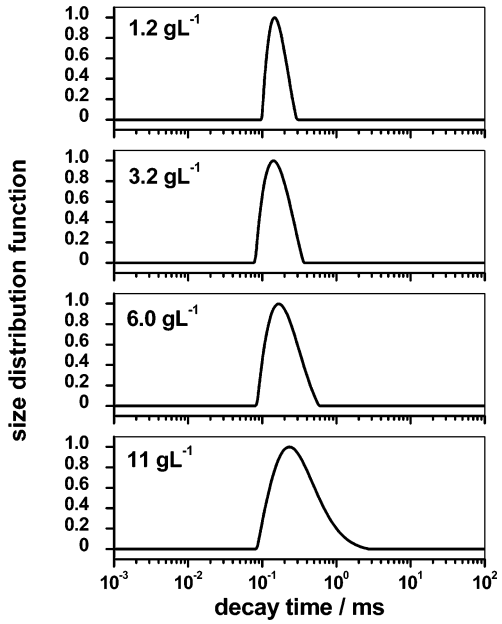

Figure 4. Decay time distributions of aqueous solutions of C_{18}-PNIPAM-C_{18}-12K of various concentrations (temperature 20 °C, Θ = 90°).

Light Scattering Study. Dynamic light scattering studies were performed on aqueous solutions of the three telechelic HM−PNIPAM samples. For C_{18}-PNIPAM-C_{18}-12K solutions of concentrations ranging from 1.2 to 11 g L^{-1}, the decay times distributions were unimodal, centered around 0.14 ms (1.2 g L^{-1}) and 0.24 ms (11 g L^{-1}) (Figure 4). Note that the distributions broaden significantly, as the polymer concentration increases. The R_H values, computed according to eq 5, increase with polymer chain length, for solutions of identical concentration (Table 2). For a given polymer, they exhibit a gradual and modest increase throughout the concentration domain probed.

The radii of gyration (R_G) of the micelles, obtained from static light scattering measurements, remain nearly constant over the 0.1−11 g L^{-1} concentration range for all samples (Table 2). From the apparent molecular weight of the polymers recorded by SLS, one can estimate the aggregation number, N_{agg}, of the micelles, expressed here in terms of number of polymer chains per micelle (Table 2). In dilute solutions, the flower micelles consist of approximately 24−27 chains for C_{18}-PNIPAM-C_{18}-12K and C_{18}-PNIPAM-C_{18}-22K. The N_{agg} value is significantly

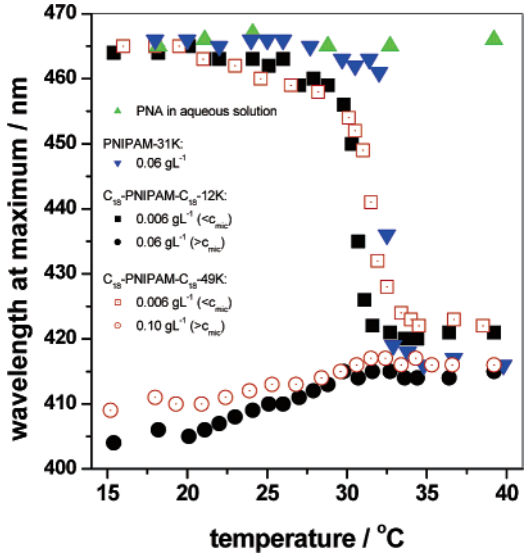

Figure 5. Changes as a function of solution temperature of the wavelength of maximum emission of *N*-phenyl-1-naphthylamine (PNA) in water and in aqueous solutions of C_{18}-PNIPAM-C_{18}-12K, C_{18}-PNIPAM-C_{18}-49K, and PNIPAM ([PNA] = 5 μM).

smaller ($N_{agg} \cong 16$ chains) in the case of the longest polymer. The R_G/R_H values of the polymeric micelles are on the order of 1.35 for C_{18}-PNIPAM-C_{18}-49K and 1.55 for the shorter telechelic HM−PNIPAMs, independently of the polymer concentration ($0.1 < c < 11$ g L^{-1}). This ratio is well-known from the Kirkwood−Riseman theory of long linear chains with hydrodynamic interactions. It takes a value of 1.504 for Gaussian chains in a Θ solvent.[38] It was also derived for star macromolecules and branched chains and shown to vary from 1.534 to 1.225 as a function of architecture for branched macromolecules in Θ conditions.[39] The lower value of R_G/R_H recorded for solutions of the longest telechelic HM−PNIPAM may indicate a more disordered arrangement of the micelles loops, compared to their shorter counterparts, as they accommodate to the crowding experienced in the vicinity of the hydrophobic core.

In summary, telechelic HM−PNIPAMs form flower micelles in dilute cold water solutions. The conformation of individual micelles and the concentration of intermicellar bridging onset depend markedly on the length of the chains carrying identical hydrophobic end groups. Short chains ($M_n \cong 12\,000$ and 22 000 g mol^{-1}) associate in the form of spherical micelles with a hydrated corona and exhibit little tendency toward intermicellar bridging, at least in solutions of concentration less that 1 wt %. They slightly grow in size as the solution concentration increases but remain spherical and hydrated, as judged from the R_G/R_H ratio. Micelles of the telechelic HM−PNIPAM sample of highest molar mass ($M_n \cong 49\,000$ g mol^{-1}) contain fewer chains and do not grow in size over the ≅0.1 to ≅11 g L^{-1} concentration range.

Temperature-Dependent Properties of Aqueous Solutions of Telechelic HM−PNIPAMs. Subjecting aqueous solutions of telechelic HM−PNIPAM to an increase in temperature triggers changes in the solubility of the polymers, and it affects the conformation of the micelle loops, as they undergo a coil-to-globule transition, leading to the formation of hydrophobic globules that may aggregate further. These processes were monitored by fluorescence and light scattering measurements carried out with solutions of the three polymer samples.

Fluorescence Probe Studies. To assess changes in the micropolarity and microviscosity within the hydrophobic domains hosting the fluorescence probe PNA, as aqueous telechelic HM−PNIPAM solutions are heated through their cloud point (T_{cp}) and the coil-to-globule collapse temperature (T_M), we measured the changes in the wavelength of maximum PNA emission as various polymer solutions were heated from 15 to 40 °C. Solutions analyzed included (i) micellar solutions of the various C_{18}-PNIPAM-C_{18} solutions ($c > c_{mic}$), (ii) C_{18}-PNIPAM-C_{18} solutions of concentration lower than c_{mic}, in which the probe resides primarily in water, (iii) a solution of unmodified PNIPAM ($M_n \cong 31\,000$ g mol^{-1}, concentration 0.06 gL^{-1}), and (iv) a solution of PNA in water.

Results are presented in Figure 5 for measurements carried out with solutions of PNA in water and in the presence of C_{18}-

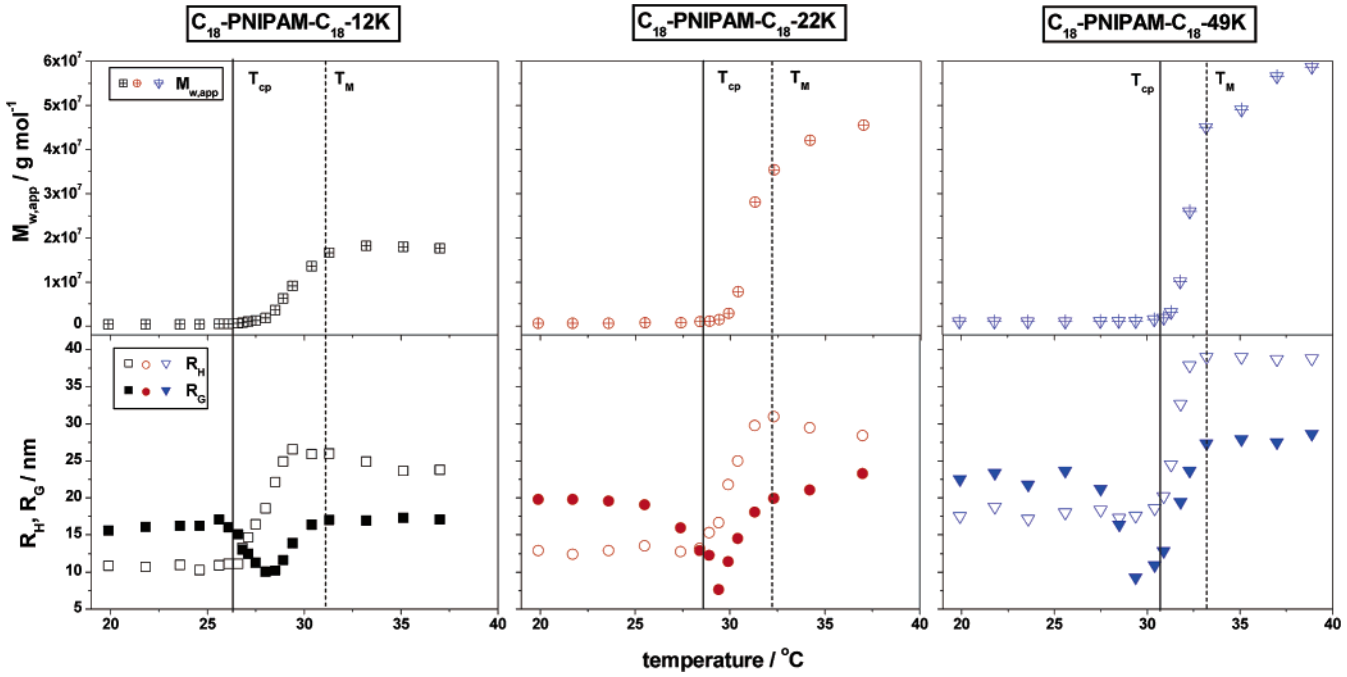

Figure 6. Changes with temperature of $M_{w,app}$ (upper panel), R_H (open symbols, lower panel), and R_G (closed symbols, lower panel) for solutions of three telechelic HM−PNIPAM (concentration: 0.3 g L^{-1}). Also indicated in the figure are the values of T_{cp} (solid lines) and T_M (dashed lines) of the various solutions, obtained from ref 20.

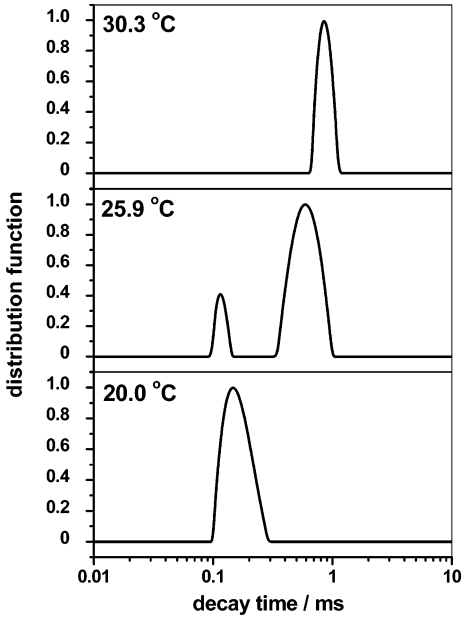

Figure 7. Decay time distributions of the autocorrelation function for aqueous solutions of C_{18}-PNIPAM-C_{18}-12K measured at 20, 25.9, and 30.3 °C (polymer concentration: 1.2 g L^{-1}, $\Theta = 90°$).

PNIPAM-C_{18}-12K, C_{18}-PNIPAM-C_{18}-49K, and PNIPAM. The wavelength of maximum emission of PNA in micellar polymer solutions underwent a gradual red shift as the solution temperature exceeded 20 °C, reaching a plateau value for solutions heated above ≅32 °C (circles in Figure 5). This shift is diagnostic of an increase in the micropolarity of the environment experienced by the probe in collapsed micelles. The PNA wavelength of maximum emission in the collapsed micelles is akin to that of the probe in ethanol (416 nm), poly(ethylene glycol) (PEG 600: 419 nm), or micelles of nonionic Brij surfactants carrying *n*-octadecyl chains (420 nm, see Table 3). The wavelength of emission maximum of the probe dissolved in premicellar polymer solutions underwent a large blue shift as the temperature exceeded ≅32 °C to reach a plateau value for $T \sim 34$ °C (squares in Figure 5). The wavelength of PNA maximum emission in the PNIPAM solution also underwent a blue shift, from 460 to 420 nm, as the solution temperature exceeded 31 °C (inverted triangles in Figure 5), signifying preferential solubilization of PNA in the hydrophobic polymer-rich phase formed. It turns out that the emission wavelength of PNA in aqueous PNIPAM ($T > 34$ °C) is the same as that recorded for PNA dissolved in telechelic HM−PNIPAM solutions of identical temperature. This similarity implies that the average micropolarity sensed by the probe is approximately the same in both cases. It is more polar than the micropolarity within the hydrophobic domains hosting the probe in hydrated flower micelles, hinting to a temperature-induced disruption of the assembly of the octadecyl end groups. Finally, note that the emission of the probe in water is not affected by changes in temperature (triangles in Figure 5).

Fluorescence depolarization measurements were carried out as well for the probe in solutions of PNIPAM and telechelic HM−PNIPAM samples kept at 35 °C, yielding the fluorescence anisotropy of PNA in the various samples (Table 3). The anisotropy of PNA emission in the collapsed micelles is significantly higher than the value recorded in cold micellar solutions, pointing to a considerable increase in the microviscosity sensed by the probe accommodated within collapsed micelles. The fluorescence anisotropy of PNA in phase-separated PNIPAM is high as well (Table 3), but it does not reach the values recorded in hot telechelic HM−PNIPAM solutions. Control experiments carried out with PNA in micellar solutions of various Brij samples (Table 3) indicate that the fluorescence anisotropy of PNA in surfactant micelle decreases with temperature, as expected given the increase with temperature of the fluidity of the surfactant micelle core.[29,40]

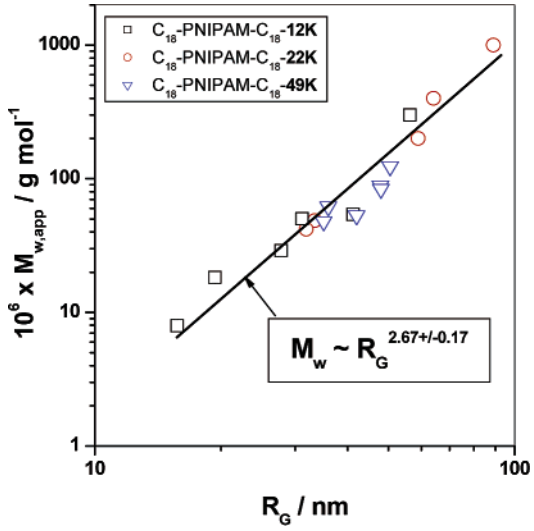

Figure 8. Scaling of the apparent molar mass of telechelic HM−PNIPAM mesoglobules $M_{w,app}$ with their radii of gyration R_G determined under equilibrium condition for solutions kept at 40 °C.

We conclude from the fluorescence experiments that the temperature-induced structural reorganization of telechelic HM−PNIPAM flower micelles leads to objects able to solubilize PNA which senses an environment more polar and more rigid than the hydrophobic core of the flower micelles formed in cold water. Light scattering experiments described next will lead us to a more precise description of these objects.

Light Scattering Studies. The temperature dependence of the apparent weight-average molar masses ($M_{w,app}$) of the telechelic HM−PNIPAM micelles (0.3 g L^{-1}) in water during a heating cycle from 18 to 40 °C are represented in Figure 6 (top). An abrupt increase in $M_{w,app}$ takes place as the solutions reach their respective cloud point temperatures. In the three cases, the growth of $M_{w,app}$ stops as the solution temperature exceeds the temperature, $T_M \sim 32$ °C, corresponding to the maximum of the endotherms recorded by DSC scans of the respective solutions.[20] The plateau $M_{w,app}$ value depends on polymer concentration. For example in the case of C_{18}-PNIPAM-C_{18}-12K, it increases by a factor of ∼10 as the solution concentration passes from 0.3 to 1.2 g L^{-1}. We note also that, as the length of the polymer increases, the enhancement of $M_{w,app}$ with temperature becomes more abrupt and spans a narrower temperature window.

The hydrodynamic radii of the flower micelles also increase sharply with solution temperature between T_{cp} and T_M (Figure 6, bottom) and reach a constant value in solutions of $T > T_M$. The R_H values determined for $T \cong 32$ °C depend strongly on polymer concentration, unlike the situation in cold solutions, for which R_H for a given polymer does not change with concentration. In the case of C_{18}-PNIPAM-C_{18}-12K, the R_H values in hot solutions nearly quadruple as the concentration passes from 0.3 to 1.18 g L^{-1}.

We noted earlier that the micellar size distributions in cold telechelic HM−PNIPAM solutions were rather broad (Figure 4). In contrast, the size distribution of the associates formed in solutions above 32 °C is remarkably narrow, as seen in Figure 7, where we represent the relaxation time distribution recorded

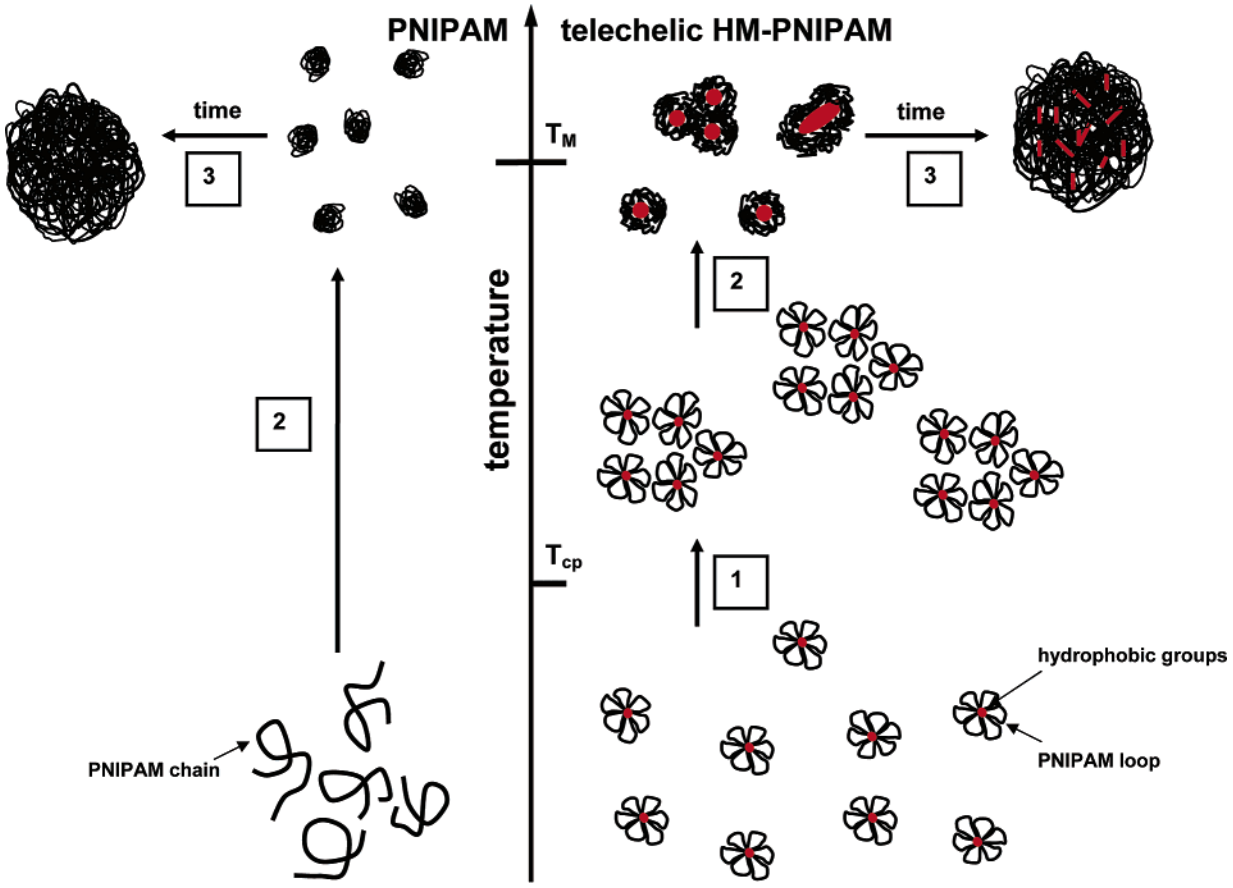

Figure 9. Pictorial representation of the temperature-induced phenomena occurring in aqueous solutions of telechelic HM−PNIPAMs (right) and PNIPAM (left) as they are heated from room temperature to $T > T_M$: 1, concentration fluctuations and intermicellar bridging; 2, collapse of PNIPAM chains; 3, mesoglobule formation.

for solutions of C_{18}-PNIPAM-C_{18}-12K (1.2 g L^{-1}) equilibrated at 20, 25.9, and 30.3 °C. The distributions are unimodal in solutions of $T < 25$ °C and $T > 30$ °C, but in the intermediate temperature domain, the situation is more complex; distributions are often bimodal, as shown in the case of a C_{18}-PNIPAM-C_{18}-12K solution kept at 25.9 °C (Figure 7, middle section). Importantly, the monodisperse associates formed above 31 °C remain stable, with no sign of further aggregation, after being kept at this temperature for several days. Thus, they present typical features of mesoglobules, defined as "equally sized spherical aggregates of more than one and less than all polymer chains colloidaly stable in solution",[23] observed in dilute solutions of PNIPAM and of various PEG-grafted PNIPAM kept above their LCST.[41−44]

Additional information on the temperature dependence of the mesoglobule structure and on the conformation of the PNIPAM loops can be gained by monitoring the changes with temperature of the radii of gyration, R_G, of telechelic HM−PNIPAMs in water. Values of R_G recorded with polymer solutions of a concentration of 0.3 g L^{-1} are presented in Figure 6 (bottom). The R_G values remain constant for $T < T_{cp}$; they decrease sharply as the solution temperature nears T_{cp}, reaching a minimum value for $T \cong T_{cp}$; then they increase gradually with temperature and attain constant values equal to, or slightly larger than, the corresponding values recorded for solutions in cold water. The decrease of R_G for telechelic HM−PNIPAM solutions near T_{cp} reflects a densification of the core of the flower micelles.

The ratio R_G/R_H of HM−PNIPAM micelles is solutions of $T > T_M$ takes a value of ∼0.80, which is close to the value characterizing a uniform solid sphere (≅0.775).[38] The ratio takes a lower value for $T_{cp} < T < T_M$, implying that aggregates of collapsed flower micelles adopt first a core−shell nanostructure, or molten globule, with a dense core formed by the hydrocarbon termini of the PNIPAM chains and a looser shell. Similar core−shell nanostructures were observed in studies of the coil-to-globule collapse of e.g. PNIPAM,[45] NIPAM−*N*-vinylpyrrolidone copolymers,[46,47] NIPAM−(styrene) multiblock copolymers,[48] and a PEO-grafted PNIPAM.[41,43,44,49] Upon heating, aggregation of individual globules takes place, the octadecyl chains being progressively solubilized within the shell of collapsed dehydrated PNIPAM loops, eventually yielding homogeneous mesoglobules that can be viewed as hard spheres.

The scaling of the apparent molar mass of the mesoglobules formed at 40 °C with R_G is presented in Figure 8. All samples follow the same law, yielding a fractal dimension of $d_f = 2.7$, a value slightly smaller than that of a hard sphere ($d_f = 3$) but significantly higher than that of coils ($d_f = 2$). It is noteworthy that the value derived from our experiments is identical to that reported by Aseyev et al. in their study of PNIPAM mesoglobules.[42] The fact that it is less than 3 implies that the globules are not fully packed and may still contain bound water.

We propose the following description of the events occurring in aqueous solutions of telechelic HM−PNIPAM heated from 15 to 40 °C, based on results of fluorescence and light scattering measurements (Figure 9, right panel). We focus here on the fate of polymer solutions that, at room temperature, exist in the form of noninteracting flower micelles. For $T < T_{cp}$, micelles consist of ≅16 (C_{18}-PNIPAM-C_{18}-49K) to 27 (C_{18}-PNIPAM-C_{18}-12K) polymer chains, the PNIPAM loops are hydrated and extended ($R_G/R_H \sim 1.35-1.55$), the micellar size distributions are unimodal and broad, and the hydrophobic core is apolar

and rigid. For $T > T_M$, stable mesoglobules, akin to hard spheres, exist in solution. The mesoglobules comprise a few hundreds chains; their interior is more rigid and more polar than the hydrophobic core of hydrated flower micelles. For $T_{cp} < T < T_M$, several phenomena occur: individual flower micelle collide and associate, possibly via formation of PNIPAM intermicellar bridges leading to high concentration fluctuations; PNIPAM loops dehydrate and collapse, and more and more micelles associate, eventually forming mesoglobules that reach an optimal size ($M_{w,app}$ constant).

Conclusions

Several recent reports point to the fact that unmodified PNIPAM in water forms stable mesoglobules at elevated temperature, at least if the solutions are sufficiently diluted, as depicted in the left-hand side of Figure 9. It is believed that two factors contribute to the stability of PNIPAM mesoglobules. They are related (1) to the general features of the spinodal decomposition of polymer solutions and (2) to the low probability of Brownian collisions in dilute solutions.[50] In a poor solvent a polymer optimizes its free energy via intermolecular association among polymer chains, which results in a decrease of the chain translational entropy. The system thus reaches a metastable state characterized by the formation of polymeric mesoglobules. Another factor contributing to mesoglobule stability, possibly a more important one, is related to the fact that the polymeric aggregates are dense and compact. Consequently, the contact time of two colliding mesoglobules may not be long enough for effective merging to occur.[51,52] It has been suggested that partial vitrification may take place within dense mesoglobules, rendering chain exchange upon merging highly unlikely.[53]

We expect that all the factors favoring the PNIPAM mesoglobular stability at elevated temperatures may be in effect also in the case of telechelic HM−PNIPAM mesoglobules. Note that effective merging of two mesoglobules, in this case, requires disentanglement of a chain bearing two hydrophobic termini, a process even less likely to occur than in the case of unmodified PNIPAM chains. The data reported here, in particular the large anisotropy of the emission of PNA in mesoglobules, strongly suggest that the rigidity, and possibly partial vitrification, of the mesoglobules may be the prevalent cause of their stability against aggregation.

Acknowledgment. This work was supported in part by a research grant of the Natural Sciences and Engineering Research Council of Canada to F.M.W., by the FQRNT Center for Self-Assembled Chemical Structures, and by the Shiseido Materials Science Consortium (F.M.W. and F.T.).

References and Notes

(1) *Hydrophilic Polymers: Performance with Environmental Acceptability*; Glass, J. E., Ed.; American Chemical Society: Washington, DC, 1996; Vol. 248.
(2) *Associative Polymers in Aqueous Solution*; Glass, J. E., Ed.; American Chemical Society: Washington, DC, 2000; Vol. 765.
(3) *Amphiphilic Block Copolymers: Self-Assembly and Applications*; Alexandridis, P., Lindman, B., Ed.; Elsevier: New York, 2000.
(4) Winnik, M. A.; Yekta, A. *Curr. Opin. Colloid Interface Sci.* **1997**, *2*, 424.
(5) Alami, E.; Almgren, M.; Brown, W.; François, J. *Macromolecules* **1996**, *29*, 2229.
(6) Chassenieux, C.; Nicolai, T.; Durand, D. *Macromolecules* **1997**, *30*, 4952.
(7) Pham, Q. T.; Russel, W. B.; Thibeault, J. C.; Lau, W. *Macromolecules* **1999**, *32*, 5139.
(8) Pham, Q. T.; Russel, W. B.; Thibeault, J. C.; Lau, W. *Macromolecules* **1999**, *32*, 2996.
(9) Beaudoin, E.; Hiorns, R. C.; Borisov, O.; François, J. *Langmuir* **2003**, *19*, 2058.
(10) François, J.; Beaudoin, E.; Borisov, O. *Langmuir* **2003**, *19*, 10011.
(11) Meng, X.-X.; Russel, W. B. *Macromolecules* **2005**, *38*, 593.
(12) Yekta, A.; Xu, B.; Duhamel, J.; Adiwidjaja, H.; Winnik, M. A. *Macromolecules* **1995**, *28*, 956.
(13) Xu, B.; Yekta, A.; Li, L.; Masoumi, Z.; Winnik, M. A. *Colloids Surf. A* **1996**, *112*, 239.
(14) Chassenieux, C.; Nicolai, T.; Durand, D.; François, J. *Macromolecules* **1998**, *31*, 4035.
(15) Beaudoin, E.; Borisov, O.; Lapp, A.; Billon, L.; Hiorns, R. C.; François, J. *Macromolecules* **2002**, *35*, 7436.
(16) Beaudoin, E.; Gourier, C.; Hiorns, R. C.; François, J. *J. Colloid Interface Sci.* **2002**, *251*, 398.
(17) Lafleche, F.; Durand, D.; Nicolai, T. *Macromolecules* **2003**, *36*, 1331.
(18) Lafleche, F.; Nicolai, T.; Durand, D.; Gnanou, Y.; Taton, D. *Macromolecules* **2003**, *36*, 1341.
(19) Kujawa, P.; Watanabe, H.; Tanaka, F.; Winnik, F. M. *Eur. Phys. J. E* **2005**, *17*, 129.
(20) Kujawa, P.; Segui, F.; Shaban, S.; Diab, C.; Okada, Y.; Tanaka, T.; Winnik, F. M. *Macromolecules* **2006**, *39*, 341.
(21) Schild, H. G. *Prog. Polym. Sci.* **1992**, *17*, 163.
(22) Okada, Y.; Tanaka, F. *Macromolecules* **2005**, *38*, 4465 and references therein.
(23) Timoshenko, E. G.; Kuznetsov, Y. A. *J. Chem. Phys.* **2000**, *112*, 8163.
(24) Timoshenko, E. G.; Kuznetsov, Y. A. *Europhys. Lett.* **2001**, *53*, 322.
(25) Timoshenko, E. G.; Basovsky, R.; Kuznetsov, Y. A. *Colloids Surf., A* **2001**, *190*, 129.
(26) Perrin, F. *Ann. Phys. (Paris)* **1929**, *12*, 169.
(27) Zhou, S.; Fan, S.; Au-Yeung, S. C. F.; Wu, C. *Polymer* **1995**, *36*, 1341.
(28) Zana, R. Luminescence probing methods. In *Surfactant Solutions: New Methods of Investigation*; Zana, R., Ed.; Dekker: New York, 1987; Vol. 22, p 241.
(29) Von Wandruszka, R. *Crit. Rev. Anal. Chem.* **1992**, *23*, 187.
(30) Winnik, F. M.; Regismond, S. T. A. *Colloids Surf. A* **1996**, *118*, 1.
(31) Preliminary measurements using a low molecular weight trithiocarbonate derivative yielded Stern−Volmer constants of $\sim 7.7 \times 10^3$ and $\sim 3.5 \times 10^3$ M^{-1} for pyrene and PNA, respectively.
(32) Brito, R. M. M.; Vaz, W. L. C. *Anal. Biochem.* **1986**, *152*, 250.
(33) Saitoh, T.; Taguchi, K.; Hiraide, M. *Anal. Chim. Acta* **2002**, *454*, 203.
(34) Yusa, S.; Fukuda, K.; Yamamoto, T.; Ishihara, K.; Morishima, Y. *Biomacromolecules* **2005**, *6*, 663.
(35) Saitoh, T.; Sakurai, T.; Kaise, T.; Matsubara, C. *Anal. Sci.* **1997**, *13* Suppl., 181.
(36) Ringsdorf, H.; Venzmer, J.; Winnik, F. M. *Macromolecules* **1991**, *24*, 1678.
(37) Claracq, J.; Santos, S.; Duhamel, J.; Dumousseaux, C.; Corpart, J. M. *Langmuir* **2002**, *18*, 3829.
(38) Burchard, W.; Schmidt, M.; Stockmayer, W. H. *Macromolecules* **1980**, *13*, 1265.
(39) Burchard, W. *Adv. Polym. Sci.* **1999**, *143*, 113.
(40) Komaromy Hiller, G.; von Wandruszka, R. *J. Colloid Interface Sci.* **1996**, *177*, 156.
(41) Virtanen, J.; Holappa, S.; Lemmetyinen, H.; Tenhu, H. *Macromolecules* **2002**, *35*, 4763.
(42) Aseyev, V.; Hietala, S.; Laukkanen, A.; Nuopponen, M.; Confortini, O.; Du Prez, F. E.; Tenhu, H. *Polymer* **2005**, *46*, 7118.
(43) Chen, H.; Zhang, Q.; Li, J.; Ding, Y.; Zhang, G.; Wu, C. *Macromolecules* **2005**, *38*, 8045.
(44) Chen, H.; Li, J.; Ding, Y.; Zhang, G.; Zhang, Q.; Wu, C. *Macromolecules* **2005**, *38*, 4403.
(45) Wang, X.; Wu, C. *Macromolecules* **1999**, *32*, 4299.
(46) Siu, M.; Zhang, G. Z.; Wu, C. *Macromolecules* **2002**, *35*, 2723.
(47) Siu, M.; He, C.; Wu, C. *Macromolecules* **2003**, *36*, 2103.
(48) Zhang, G.; Winnik, F. M.; Wu, C. *Phys. Rev. Lett.* **2003**, *30*, 35506.
(49) Hu, T.; Wu, C. *Phys. Rev. Lett.* **1999**, *83*, 4105.
(50) Aseyev, V.; Tenhu, H.; Winnik, F. M. In *Self-Organization of Amphiphilic Copolymers in Aqueous Media*; Khokhlov, A. R., Ed.; Springer-Verlag GmbH: Heidelberg, Germany, in press.
(51) Tanaka, H. *Macromolecules* **1992**, *25*, 6377.
(52) Picarra, S.; Martinho, J. M. G. *Macromolecules* **2001**, *34*, 53.
(53) Van Durme, K.; Verbrugghe, S.; Du Prez, F. E.; Van Mele, B. *Macromolecules* **2004**, *37*, 1054.

MA0600254